THE ASTROPHYSICAL JOURNAL, 537:916–921, 2000 July 10


# THEORETICAL TRANSMISSION SPECTRA DURING EXTRASOLAR GIANT PLANET TRANSITS

S. SEAGER[1] AND D. D. SASSELOV[2,3]

*Received 1999 December 7; accepted 2000 February 7*

## ABSTRACT

The recent transit observation of HD 209458 b—an extrasolar planet orbiting a Sun-like star—confirmed that it is a gas giant and determined that its orbital inclination is 85°. This inclination makes possible investigations of the planet atmosphere. In this paper we discuss the planet transmission spectra during a transit. The basic tenet of the method is that the planet atmosphere absorption features will be superimposed on the stellar flux as the stellar flux passes through the planet atmosphere above the limb. The ratio of the planet's transparent atmosphere area to the star area is small ($\sim 10^{-3}$ to $10^{-4}$); for this method to work, very strong planet spectral features are necessary. We use our models of close-in extrasolar giant planets to estimate promising absorption signatures: the alkali metal lines; in particular, the Na I and K I resonance doublets; and the He I 2 $^3S$–2 $^3P$ triplet line at 1083.0 nm. If successful, observations will constrain the line-of-sight temperature, pressure, and density. The most important point is that observations will constrain the cloud depth, which in turn will distinguish between different atmosphere models. We also discuss the potential of this method for extrasolar giant planets at different orbital distances and orbiting nonsolar-type stars.

*Subject headings:* planetary systems — radiative transfer — stars: atmospheres

## 1. INTRODUCTION

The recent transit detection of HD 209458 b (Charbonneau et al. 2000; Henry et al. 1999, 2000a) concludes a period of eager anticipation since the first close-in extrasolar giant planet (CEGP), 51 Peg b, was discovered in 1995 (Mayor & Queloz 1995). Five close-in extrasolar giant planets with orbital radii $\leq 0.05$ AU are known, and there are an additional six closer than 0.15 AU.[4] The chance of a transit for a CEGP—assuming random alignment of the orbital inclination—is roughly 10%. Transits have been excluded for five of the 11 above planets (Henry et al. 2000b, 1997; Baliunas et al. 1997; G. Henry, 1999 private communication). The transit of HD 209458 b confirms that the CEGPs are gas giants, gives the planet radius, and fixes the orbital inclination, which removes the sin $i$ ambiguity in mass and provides the average planet density.

While the transit gives important physical parameters for the planet, it cannot provide any information about the planet's atmosphere. Nevertheless, the near edge-on orbital inclination means that HD 209458 b is promising for a number of different types of planet atmosphere investigations. Two of these involve optically reflected light and benefit from the nearly full phase of the planet: spectral separation of the combined star-planet light (Cameron et al. 1999; Charbonneau et al. 1999) and photometric observations of the phase curve from reflected planetary light (see Seager, Whitney, & Sasselov 2000 for a full discussion.) A third method is the transmission spectra discussed here, which requires the near edge-on orientation.

Observations of spectra in transmission are not new: they have been observed in binary stars (e.g., Eaton 1993), they have been extensively observed and analyzed for occultations of stars and the Sun by planets in our solar system (e.g., Smith & Hunten 1990), they are one motivation for large transit surveys of stars with no known CEGPs (e.g., Vulcan Camera Project [PI W. Borucki], STARE [PI T. Brown], WASP [PI S. Howell]), they have been discussed briefly for extrasolar planets (e.g., Schneider 1994; Charbonneau et al. 2000), and they have been discussed for extrasolar planet exospheres (Rauer et al. 2000). Here, for the first time to our knowledge, we quantify the method for CEGPs and provide estimates of specific spectral features in the combined star-planet light during a planet transit. Many more CEGPs will be detected in the near future, both by ongoing radial-velocity searches and by wide-field transit searches. The transit transmission lines will provide us with constraints on cloud top location and line-of-sight column density, temperature ($T$), and pressure ($P$).

## 2. TRANSMISSION SPECTRA

During an EGP planetary transit, the planet passes in front of the star and occults the stellar flux in the amount equal to the ratio of the planet-to-star area. During the transit, some of the stellar flux will pass through the optically thin part of the planet atmosphere, the part of the atmosphere above the planet limb. In stellar occultations by planets in the solar system, the limb of giant planets is usually defined at (1) the cloud tops or (2) the 1 bar level (Atreya 1986). Here we define the planet limb as the boundary (e.g., the cloud tops) above which the planet's atmosphere is transparent to the stellar continuum radiation. The clouds are taken to be 1 pressure scale height above the cloud base, which due to irradiation heating is expected to be well above the 1 bar level (Seager 1999). We call the entire atmosphere above the limb the "transparent atmosphere," although the transparent atmosphere is optically thick in some transitions. Below the limb the optically thick clouds prevent radiation from being transmitted through the atmosphere.

The ratio of the planet's projected transparent atmosphere area to star-minus-planet area is small, on the order of $10^{-4}$ to $10^{-3}$, using $R_* = 1.3\,R_\odot$, $R_P = 1.54 R_J$ (based on HD 209458 parameters from Mazeh et al. 2000) and using an estimate for the limb radial depth of $0.01R_P$–$0.05R_P$.

[1] Postal address: School of Natural Sciences, Institute for Advanced Study, Olden Lane, Princeton, NJ 08540.

[2] Astronomy Department, Harvard University, 60 Garden Street, Cambridge, MA 02138.

[3] Alfred P. Sloan Research Fellow.

[4] Schneider, J. 1999, http://cfa-www.harvard.edu/planets/.

The planet's absorption features will be superimposed on the observable stellar flux and will appear at the $\sim 10^{-4}$ level below the continuum flux. Very strong spectral features are needed for detection; essentially, the absorption features must be optically thick. In contrast to reflected planetary light, the transit transmission flux is not diluted by the planet-star distance and is not cloud albedo dependent.

During solar system planet occultations and binary star occultations, successive measurements are made as the planet occults the star (i.e., during ingress or egress). The time-dependent change in spectral features provides column density and temperatures for different atmosphere heights. Because the CEGP is much smaller and fainter than the parent star, this will not be possible in the near future. The best orbital phase for the transmission spectra observations of CEGPs is when the planet is fully projected on the visible hemisphere of the star so that the planet's projected transparent atmosphere takes out the greatest area and limb darkening from the star is at its minimum.

Refraction through the CEGP's atmosphere has to be accounted for in defining the limb and in computing the total optical path of rays reaching us through it. During the solar transit of Venus in 1761, an obvious refraction effect at second contact convinced Lomonosov in St. Petersburg that Venus had an atmosphere (Cruikshank 1983). However, the cloud tops in our model of HD 209458 b (see below) are high in its atmosphere, where the gas density is fairly low and refraction is small. In an isothermal atmosphere with gas scale height $H$, the angle of refraction for a ray passing at planetocentric distance $r$ is $\theta = \nu(r)[(2\pi R_P)/H]^{1/2}$, where $\nu(r) = n - 1$ is the atmospheric refractivity at $r$ (for an $H_2$+He mixture at STP: $\sim 1.2 \times 10^{-4}$) with $n(\lambda, r)$ the index of refraction. Refraction introduces a lengthening of the pathways of the rays through a spherical stratified atmosphere: $\Delta s = 0.5z\theta^2$, where simply $z^2 = (R_P + H)^2 - R_P^2$. Unlike stellar occultations in our solar system, in CEGP transits the parent star is a very extended background source and subtends a significant solid angle at its orbit. This allows us to observe rays deflected at angles larger than the average isothermal $\theta$ through the densest optically thin layers of the atmosphere. However, the cloud tops in HD 209458 b are still at $P < 10^5$ dyn cm$^{-2}$ and $\Delta s/s < 2\%$.

### 2.1. *Close-in EGPs Transparent Atmosphere Model*

We consider the only currently known EGP system with an observed transit, HD 209458. We use the stellar parameters $R_* = 1.3\ R_\odot$, $T_{\rm eff} = 6000$ K, $\log g = 4.25$, and [Fe/H] = 0.0, derived from evolutionary calculations and fits to spectroscopic data in Mazeh et al. (2000). We use the planetary parameters $R_P = 1.54R_J$, $M_P = 0.69M_J$, $\log g = 2.9$, and $i = 85.^\circ 2$, derived from the transit observations and radial velocity observations, together with the stellar parameters (Mazeh et al. 2000). For a circular orbit, we derive a semimajor axis $a = 0.0468$ AU. We compute the incident flux of HD 209458 with the above parameters from the model grids of Kurucz (1992).

We compute the CEGP atmosphere (temperature-pressure [$T$-$P$] profile and emergent spectra) using our code described in Seager (1999) and Seager et al. (2000). This code is improved over the version described in Seager & Sasselov (1998) in two major ways. One is a Gibbs free energy minimization code to calculate solids and gases in chemical equilibrium; the second is condensate opacities for three solid species. So while in Seager & Sasselov (1998) we considered neither the depletion of TiO nor formation of $MgSiO_3$, in the new models we do. One of the largest uncertainties in the atmosphere models is the location of clouds, as well as the cloud particle type and size. In Seager et al. (2000), we find that the $T$-$P$ profile and the emergent flux (reflected + thermal) depends entirely on the condensate assumptions.

Because we define the planet limb at the cloud tops, the cloud wavelength-dependent albedos are not directly important. Furthermore, even if the clouds were not optically thick, they would not superimpose any spectral features on the optical stellar flux since their extinction (absorption + scattering) is generally a smooth function of wavelength.

#### 2.1.1. *Transparent Atmosphere Temperature-Pressure Profile*

We use the radial $T$-$P$ profile generated in the self-consistent irradiated atmosphere code and construct a limb depth and line-of-sight $T$-$P$ profile from geometrical considerations. The limb of the planet, as defined above, is approximately 0.01 $R_P$. Together with $R_P = 1.54R_J$ and $R_* = 1.3\ R_\odot$, this thickness gives a ratio of the projected transparent atmosphere to the stellar disk of $3.6 \times 10^{-4}$. The line-of-sight $T$-$P$ profile describes a plane-parallel column of gas through which the stellar flux passes. The gas is optically thin; flux at most wavelengths passes through relatively unattenuated. We compute the sum through several line-of-sight columns of gas, from the densest column tangential to the cloud top to the column that just skims the uppermost atmosphere. However, in an atmosphere with exponential density falloff, almost all of the absorption occurs in the densest column.

To solve for the radial atmosphere structure, we must make a specific assumption about cloud particle type and size. Here we consider 10 $\mu$m grains of $MgSiO_3$, Fe, and $Al_2O_3$. For this particular model ($T_{\rm eff} = 1350$ K), the transparent atmosphere above the limb is comprised of a gas between 850 and 1000 K with pressures 20–600 dyne cm$^{-2}$. The main constituents of a gas at these temperatures and pressures are $H_2$, CO, $H_2O$, and He. Because of the irradiative heating, CO dominates over $CH_4$ in this CEGP model. Most gases are in molecular form with the exception of He and the alkali metals. The volatile elements (e.g., Mg, Ca, Ti) have condensed into grains, and we assume they have settled to within 1 pressure scale height of the cloud base. Photochemistry is not included, but the UV radiation from the parent star could photoionize a small fraction of $H_2$, CO, etc., through the transparent atmosphere. This, however, would have little consequence on the results (see § 2.2.3).

#### 2.1.2. *Cloud Models*

We caution that the transmission spectra presented here are estimates that depend on several assumptions. Once observations are successful, a more careful computation to accurately interpret the data is necessary. One point to make is that the location of the cloud base—and hence the cloud tops—depends on the irradiative heating of the planet atmosphere, which itself depends heavily on the absorptivity of the type and size of condensates present throughout the planet atmosphere. A model with absorptive grains causes the upper atmosphere temperature to be

higher compared to a model with highly reflective grains, and the grain condensation boundary will be closer to the top of the planet atmosphere. In the model used here, we consider 10 $\mu$m grains of $MgSiO_3$, Fe, and $Al_2O_3$. While the $MgSiO_3$ clouds are the highest in the atmosphere, all are important for computing the irradiated $T$-$P$ profile. The choice of cloud particle type and size distribution is highly uncertain; this is the most complex free parameter of the models. In Seager et al. (2000), we discuss this in more detail.

Another major assumption used is that the radial $T$-$P$ profiles are similar on all parts of the planet. This would be the case if strong winds redistribute the heat efficiently (e.g., as on Jupiter where there is no apparent difference from one side of the terminator to the other.) A different line-of-sight $T$-$P$ profile does not change our predictions much; the flux ratio is set by the planet limb, star area, and planet area, and the features are superimposed on that. Indeed, it is very difficult to predict the exact line shape with so many unknowns about the planet atmosphere such as element abundances (from both planet metallicity and nonequilibrium chemistry) and cloud location due to heating.

### 2.2. *Results*

The CEGP and parent solar-type star have almost no spectral features in common; at effective temperatures ($T_{\rm eff}$) ranging from $\sim$1100 to $\sim$1600 K, the CEGPs are almost 5 times cooler than the stars at $T_{\rm eff}$ = 5000–6000 K. Thus, the transmission spectra method is promising. In this subsection we discuss strong signals in the planetary atmosphere.

#### 2.2.1. *Alkali Metals*

The Na I and K I resonance doublets are predicted to be strong in CEGPs (Seager et al. 2000; Sudarsky, Burrows, & Pinto 2000), assuming the atmospheres are similar to brown dwarfs and cool L dwarfs which have similar $T_{\rm eff}$ values. Alkali metals have clear signatures in cool L dwarfs and brown dwarfs where the metals such as Ti have condensed out of molecular form into solids, depleting the strong optical molecular absorbers. The K I doublet 4 $^2S$–4 $^2P$ absorption line at 767.0 nm is extremely broad in methane dwarfs, such as Gliese 229B, which have $T_{\rm eff}$ values a few hundred degrees lower than the CEGPs. The broad wings of the K I resonance doublet extend for several tens of nanometers and are responsible for the large continuum depression in the optical and flux slope redward to 1 $\mu$m (Tsuji, Ohnaka, & Aoki 1999; Burrows, Marley, & Sharp 2000). The broad lines are caused by strong pressure broadening by $H_2$ and are in part so prominent because there are no other strong absorbers present at those wavelengths throughout the entire atmosphere. There is some question about the shape of the alkali metal lines in the CEGP atmospheres; they will be very broad if the clouds are low in the atmosphere and the large pressures deep in the atmosphere can contribute to strong line broadening. Sudarsky et al. predict this scenario, where K I and Na I absorb essentially all incoming optical radiation redward of 500 nm. Sudarsky et al. use ad hoc modified $T$-$P$ profiles, to simulate heating, which have clouds at the 10 bar level. Seager et al. (2000) include heating from the parent star on the $T$-$P$ profile and find that the lines are much narrower since clouds exist higher in the atmosphere at lower pressure. Observations should be able to distinguish between the two cases.

With the columns of gas defined above (§ 2.1.1), we compute the attenuation of the incoming intensity with the radiative transfer equation in the limit of no scattering $I(\nu, z) = I_*(\nu, z) \exp[-\kappa(\nu, z)]$, where $I_*(\nu, z)$ is the stellar intensity, $\nu$ is the frequency, and $z$ is the depth along the line of sight through the planet's transparent atmosphere. Here $\kappa(\nu, z)$ is the extinction which includes absorption and scattering. Our code includes the dominant opacities expected for cool L dwarfs and brown dwarfs: $H_2O$, TiO, $CH_4$, $H_2$-$H_2$ and $H_2$-He collision-induced opacities, Rayleigh scattering from H, He, $H_2$, and the alkali metal lines. The oscillator strengths and energy levels for the lower levels of the alkali metals (Na, K, Li, Rb, Cs) were taken from Radzig & Smirnov (1985) and the Kurucz atomic line list (Kurucz & Bell 1995), and we compute line broadening using a Voigt profile with $H_2$ and He broadening and Doppler broadening. We do not need to solve the full radiative transfer equation since we assume the effect of transmitted intensity through the planet's transparent atmosphere is negligible with regard to the radiative structure which is already accounted for in the irradiation model.

Figure 1 shows the flux from the star and the stellar flux that has passed through the planet's transparent atmosphere. The curves are essentially the same in the UV through the optical, with the exception of the absorption lines, including Na I at 285.4 nm and 342.8 nm, the Na I resonance doublet at 589.4 nm, and the K I resonance doublet at 767.0 nm. The He I triplet line is at 1083 nm. In the infrared, the stellar flux is absorbed by the water bands, as well as the 5 $\mu$m and the 3.3 $\mu$m methane band (not visible in the figures). No molecular features such as TiO appear in the spectra since those molecules have been depleted into solids. Solar-type stars also have alkali metal lines, but they are weak because most of the alkali metals are ionized. In addition, the stellar optical spectrum is crowded with other atomic absorption lines.

Figure 2 shows the normalized in-transit minus out-of-transit spectra, i.e., the transmission spectra as the percentage occulted area of the star at different wavelengths. In

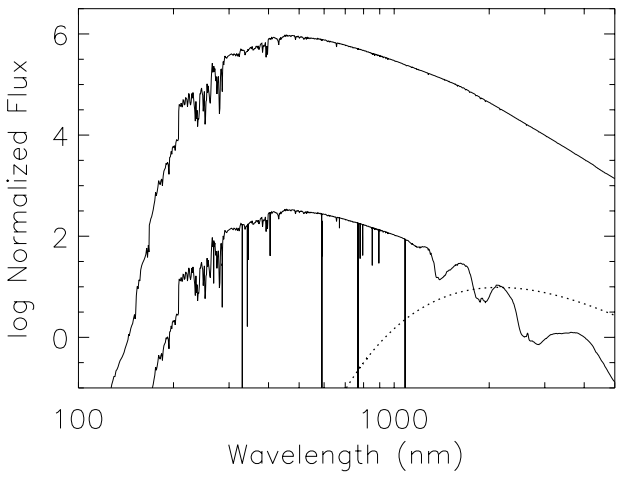


FIG. 1.—Flux of HD 209458 a (*upper curve*) and the transmitted flux through the planet's transparent atmosphere (*lower curve*). Superimposed on the transmitted flux are the planetary absorption features, including the He I triplet line at 1083 nm. The other bound-bound lines are alkali metal lines (see Fig. 2 for details). The $H_2O$ and $CH_4$ molecular absorption dominates in the infrared. The dotted line is a blackbody of 1350 K representative of the CEGP's thermal emission, but the thermal emission can be larger than a blackbody blueward of 2000 nm.

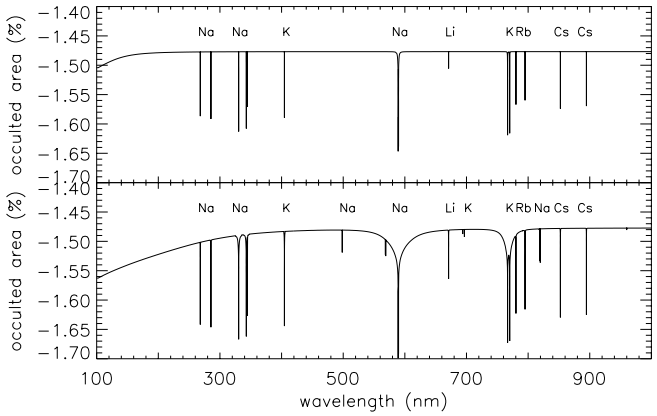


FIG. 2.—*Upper plot*: The normalized in-transit minus out-of-transit spectra, i.e., percent occulted area of the star. In this model the cloud base is at $2.4 \times 10^{-3}$ bar. Rayleigh scattering is important in the UV. *Lower plot*: A model with cloud base at 0.2 bar. The stellar flux passes through higher pressures, densities, and temperatures of the planet atmosphere compared to the model in the upper plot. In addition, a larger transparent atmosphere makes the line depth larger. Observations will constrain the cloud depth. See text for discussion.

transmitted light the planet is different sizes at different wavelengths. The zero point (at $\sim -1.47\%$) is set by the atmosphere depth at which the planet is optically thick at all wavelengths (the observed transit). The planet appears largest in the line cores, where photons passing very high in the planet atmosphere are still absorbed along the line of sight due to the strong absorption by the Na I and K I resonance lines. This figure differs from the model in Figure 1 in that we have considered the atmosphere out to the distance where the Na I resonance line becomes optically thin along the line of sight. In this case the limb depth is several percent of $R_P$ (where the limb coincides with the observed transit). Rayleigh scattering from $H_2$ is important below 200 nm; otherwise, it is negligible. The Na I resonance doublet is broader than the K I resonance doublet because its abundance is an order of magnitude higher.

Figure 2 also shows the transmission spectra from an atmosphere with a cloud base much deeper than predicted by our model, at 0.2 bar instead of at $2.4 \times 10^{-3}$ bar. (We note that in our range of models for different condensate type and size the highest clouds have bases ranging from roughly 0.5 to $10^{-3}$ bar.) There will be two main consequences. First, the transparent atmosphere area will be larger, resulting in the total line depths being larger with respect to the zero point. Exospheric escape or photoionization by stellar UV radiation could affect the line cores. Second, the stellar flux will pass through higher densities, pressures, and temperatures. Rayleigh scattering is strong in this relatively high density transparent atmosphere. When higher pressures are sampled by the transmitting photons, the lines become more pressure-broadened. This is seen in the Na I and K I resonance doublets. The higher densities will cause stronger alkali lines and additional absorption lines from other transitions that were too weak to appear in the low densities of our line-of-sight model, for example, nonresonance lines of Na I and K I. Observations of the alkali metal lines will be able to constrain cloud location.

### 2.2.2. *Neutral Helium*

We expect a strong absorption line at 1083 nm due to scattering of background stellar photosphere photons off the overpopulated He atoms excited to the triplet $2\ ^3S$ metastable state. The mechanism works as follows. The stellar EUV radiation shortward of 50.4 nm will photoionize neutral He atoms, and they will recombine at the local kinetic temperature, which may be as low as 800 K in the upper atmosphere of the planet. The He I recombination cascade is efficient for the singlet states but stops at $2\ ^3S$ for the triplet states which lack a fast radiative decay path to the ground state. Due to the low local kinetic temperature, collisional de-excitation is negligible. On the other hand, the number of 1083 nm continuum photons from the G0 V star is very large—they scatter efficiently in the $2\ ^3S$–$2\ ^3P$ transition and produce the strong absorption feature in the transmission spectrum.

Versions of this mechanism are responsible for enhanced He I 1083 nm absorption in solar spectra (Zirin 1975; Andretta & Jones 1997), Algol binary systems (Zirin & Liggett 1982), etc. In the case of HD 209458, a Sun-like star, we assume the EUV radiation to be that of the Sun (from Tobiska 1991). We use the $T$-$P$ distribution of the transparent atmosphere generated in the Seager & Sasselov code and illuminate it with that diluted EUV field, simultaneously solving the non-LTE transfer for a helium model atom with singlet and triplet states up to $n = 4$. The details of this calculation are essentially the same as in Sasselov & Lester (1994). One has to realize that this calculation is more an estimate than a fully consistent treatment of He I 1083 nm line formation in the unusual conditions of the EGP's atmosphere. However, the mechanism described above is very robust, and given no other competing target(s) for the EUV photons except H and $H_2$ the $2\ ^3S$–$2\ ^3P$ transition is optically thick at line center. In fact, He (and H) is prone to creating an extended exosphere around the planet; if so, the strength of the He I 1083.0 nm absorption may well be extremely great (due to a much larger transparent atmosphere) and easy to observe. The broadening of the line ($\sim 0.3$ nm) is not significant, but this needs further study in terms of He collisional broadening by molecular species like $H_2$.

In the spectrum of the inactive parent star, the He I 1083.0 nm triplet line is extremely weak, if it is present at all. This makes it a promising signature in the combined planet-star flux. Enhanced absorption of the $3\ ^3P$–$3\ ^3D$ transition of C is also seen in binary systems, but in the CEGP atmospheres the C is locked in CO or $CH_4$.

### 2.2.3. *UV and Infrared Wavelengths*

Solar system outer planet occultation transmission lines have been very successfully observed in the UV where the molecules such as $H_2$, $N_2$, and $O_2$ have strong absorption signatures. In addition, in CEGPs the H resonance line transitions are strong (and may be enhanced by photodissociation of $H_2$) and alkali metal resonance line absorption appears in the near-UV (Fig. 2). For the CEGPs orbiting Sun-like stars, the UV flux is very low, and the lines—while useful diagnostics—will be difficult to detect.

The spectral transmission signatures in the infrared (e.g., $H_2O$ and $CH_4$) shown in Figure 1 will be difficult to distinguish from the planet's own thermal emission, which is present at all phases. More importantly, redward of 2000 nm the planet's thermal emission, which roughly follows a blackbody (dotted line in Fig. 1), will be much stronger than the transmitted spectrum that follows the optical-peaking stellar spectrum. This is in contrast to the optical where the

planet has no emission; during transit the optical transmission spectrum is the planet's only contribution to the total flux. Blueward of 2000 nm the transmission spectrum may be brighter than the planet's own emission, and for the $2.4 \times 10^{-3}$ bar cloud base model observations in this region may be very promising. (Note that for some models the planet's thermal emission can be much higher than a blackbody in that region [Seager 1999].) Nevertheless, $CH_4$ is an important temperature diagnostic because the temperature-pressure profiles of the CEGPs fall near the $CO/CH_4$ equilibrium curve (Seager 1999; Goukenleuque et al. 1999). The strength of the methane absorption could indicate the temperature in the planet's upper atmosphere layers, which in turn will distinguish between different irradiated models.

In principle, the infrared magnitude of the brightness of the planet will increase slightly just after first contact as illumination passes through the top of the transparent atmosphere, but against the backdrop of the star this will not be detectable. CO (not included in this model) may also be good transmission signatures in the infrared.

#### 2.2.4. *Comparison of Spectra Using Different $R_P$ and $R_*$*

We have also run calculations using $R_P = 1.27$ (and $i = 87°$) from Charbonneau et al. (2000), who assumed $R_* = 1.1$. In this case the ratio of planet-to-star area is slightly lower ($\sim 5\%$) than with the correct values due to the higher inclination. In our self-consistent models, the effect of a smaller planet radius and smaller stellar radius decreases the transmitted-to-stellar flux ratio by an even smaller amount. The reason is that a smaller star and planet means the star-planet distance is larger, making the planet's atmosphere slightly cooler. The cooler atmosphere has the $MgSiO_3$ cloud top lower in the atmosphere and hence has a larger transparent atmosphere area compared to the hotter model. For example, the equilibrium effective temperature is $T_{eq} = T_*(R_*/2D)^{1/2}(1 - A)^{1/4}$, where $T_*$ is the effective temperature of the star and $A$ is the Bond albedo. Because $T_{eq} \sim R_*^{1/2}$, decreasing $R_*$ from 1.3 to 1.1 $R_\odot$ will change the planet's $T_{eq}$ by $\sim 100$ K.

There is also a small change due to density. At the same optical depth, the smaller radius planet with a higher surface gravity will have a higher density compared to the planet with a larger radius. Thus, in comparison the absorption lines will be slightly stronger for the same optical depth.

## 3. OTHER EGPs

As of this writing there are 29 known extrasolar planets around 27 stars. The value of $M$ sin $i$ ranges from 0.42 to 11 $M_J$ and planet-star distances from 0.042 to 2.5 AU. In principle, observations of the transmission features of any transiting planet can be attempted. Many of the stars are being monitored for transits, and transits around several of these stars have been excluded (Henry et al. 1997, 2000b; Baliunas et al. 1997). Three others of these known planet systems have their inclinations limited by observation of Kuiper belt–like disks (Trilling, Brown, & Rivkin 1999). Wide-field transit searches are excluded to transiting systems and are mostly sensitive to systems with orbital distances below 0.2 AU.

CEGPs much more massive than HD 209458 b will have a much smaller transparent atmosphere area. The planet radius is a weak function of mass (Guillot et al. 1996), and more massive planets are expected to be more compact as the degenerate core increases at the expense of the gaseous atmosphere. For a more massive planet with all other parameters equal (atmosphere structure, radius, etc.), the scale height is smaller, and defined by optical depth the entire atmosphere including the transparent atmosphere is smaller. For example, $\tau$ Boo b, which has $M$ sin $i = 3.87$ (Butler et al. 1997), is at least 5.6 times more massive than HD 209458 b. CEGPs with higher $T_{eff}$ values than HD 209458 b (e.g., $\tau$ Boo b) may have cloud bases closer to the top of the atmosphere, also resulting in a smaller transparent atmosphere area. The flux ratio of transmitted to total stellar flux is also sensitive to the stellar radius and would change by a factor of 3 for solar-type parent stars; from evolutionary calculations (Ford, Rasio, & Sills 1999), the solar-type parent stars of known CEGPs with orbital distances below $\sim 0.2$ AU range from 0.93 to 1.56 $R_\odot$.

Wide-field transit searches will find short-period planets orbiting stars where radial velocity planet detections are not possible, for example, around active cool stars and hot stars that have rotationally broadened atomic lines and activity. The parent stars of known EGPs range from F6 IV ($\tau$ Boo) down to M4 V (Gliese 876). Planet transmission spectra may be difficult to disentangle from parent M stars whose optical spectra are very crowded with molecular lines such as TiO and VO. Nevertheless, because of the larger planet-to-star area ratio the flux ratio is enhanced by a factor of $\sim 10$. Jupiter-sized planets orbiting hot stars such as a B or O star would have a flux ratio decreased compared to solar by a factor of 10–100, but the UV flux (observed from space) would provide many useful molecular absorption signatures such as $H_2$, $N_2$, and $O_2$.

## 4. SUMMARY AND PROSPECTS

We have estimated the transmission spectra of a CEGP during an occultation of the parent star. We find very strong absorption signatures of Na I and K I and a strong signature of the He I $2\ ^3S$–$2\ ^3P$ triplet line at 1083.0 nm. We find the number, strength, and depth of spectral features are sensitive to the cloud top depth in the planet atmosphere.

Detecting spectral features will require high-resolution, high–signal-to-noise observations (e.g., with Keck HIRES). During the transit of HD 209458, the Doppler shift of the planet is strong enough so that it should be taken into account when analyzing the spectra. Spectral separation techniques, designed to detect absorption signatures at the less than $10^{-4}$ level (e.g., Cameron et al. 1999; Charbonneau et al. 1999) may be necessary to recover the weak planet signal. Systematic red or blue shifting from winds blowing between the day and night side may have a detectable effect on the planet spectrum (D. Charbonneau & T. Brown 1999, private communication). Measurements of metallic lines will also constrain (together with $M_P$, $R_P$, and $\rho_P$) the interior models and shed light on the formation scenario of CEGPs, e.g., core accretion versus gravitational disk instability. The CEGP's extended exosphere may be easy to detect in the He 1083.0 nm transition.

If successful, observations of transmission spectra will be the first made of an extrasolar planet atmosphere and will provide constraints on the upper atmosphere column density, temperature, and pressure. In addition, the observations should easily constrain the cloud top depth, which naturally defines the planet limb. This information will help distinguish between atmosphere models. Most importantly,

detection of the alkali metal absorption lines will confirm the very basic postulate that the CEGPs have similar atmospheres to those of methane dwarfs and cool L dwarfs which have similar $T_{\rm eff}$ values.

We are grateful to Dave Latham for providing the stellar and planet parameters for the HD 209458 system before publication. We thank Bob Noyes, Tim Brown, and Mark Marley for reading the manuscript and for helpful comments and discussion. We also thank Dave Charbonneau and Avi Loeb for useful discussions. S. S. is supported by NSF grant PHY-9513835. D. D. S. acknowledges support from the Alfred P. Sloan Foundation.

REFERENCES

Andretta, V., & Jones, H. P. 1997, ApJ, 489, 375
Atreya, S. 1986, Atmospheres and Ionospheres of the Outer Planets and Their Satellites (New York: Springer)
Baliunas, S. L., Henry, G. W., Donahue, R. A., Fekel, F. C., & Soon, W. H. 1997, ApJ, 474, L119
Burrows, A., Marley, M., & Sharp, C. 2000, ApJ, 531, 438
Butler, R. P., Marcy, G. W., Williams, E., Hauser, H., & Shirts, P. 1997, ApJ, 474, L115
Cameron, C. C., Horne, K., Penny, A., & James, D. 1999, Nature, 402, 751
Charbonneau, D., Brown, T., Latham, D., & Mayor, M. 2000, ApJ, 529, L45
Charbonneau, D., Noyes, R. W., Korzennik, S. G., Nisenson, P., Jha, S., Vogt, S. S., & Kibrick, R. 1999, ApJ, 522, L145
Cruikshank, D. P. 1983, in Venus, ed. D. Hunten, L. Colin, T. Donahue, & V. Moroz (Tucson: Univ. Arizona Press), 1
Eaton, J. A. 1993, ApJ, 404, 305
Ford, E. B., Rasio, F. A., & Sills, A. 1999, ApJ, 514, 411
Goukenleuque, C., Bézard, B., Joguet, B., Lellouch, E., & Freedman, R. 2000, Icarus, 143, 308
Guillot, T., Burrows, A., Hubbard, W. B., Lunine, J. I., & Saumon, D. 1996, ApJ, 459, L35
Henry, G., Marcy, G., Butler, P., & Vogt, S. 1999, IAU Circ. 7307, 1
———. 2000a, ApJ, 529, L41
Henry, G. W., Baliunas, S. L., Donahue, R. A., Fekel, F. C., & Soon, W. 2000b, ApJ, 531, 415
Henry, G. W., Baliunas, S. L., Donahue, R. A., Soon, W. H., & Saar, S. H. 1997, ApJ, 474, 503
Kurucz, R. 1992, in IAU Symp. 159, Stellar Population of Galaxies, ed. B. Barbuy & A. Renzini (Dordrecht: Kluwer), 225
Kurucz, R. L., & Bell, B. 1995, CD-ROM 23, Atomic Line Data (Cambridge: SAO)
Mayor, M., & Queloz, D. 1995, Nature, 378, 355
Mazeh, T., et al. 2000, ApJ, 532, L55
Radzig, A. A., & Smirnov, B. M. 1985, Reference Data on Atoms, Molecules, and Ions (New York: Springer)
Rauer, H., Bockelée-Morvan, D., Coustenis, A., Guillot, T., & Schneider, J. 2000, A&A, 355, 573
Sasselov, D. D., & Lester, J. B. 1994, ApJ, 423, 785
Schneider, J. 1994, Ap&SS, 212, 321
Seager, S. 1999, Ph.D. thesis, Harvard Univ.
Seager, S., & Sasselov, D. D. 1998, ApJ, 502, L157
Seager, S., Whitney, B. A., & Sasselov, D. D. 2000, ApJ, in press (preprint astro-ph/0004001)
Smith, G. R., & Hunten, D. M. 1990, Rev. Geophys., 28, 117
Sudarsky, D., Burrows, A., & Pinto, P. 2000, ApJ, in press (preprint astro-ph/9910504)
Tobiska, W. K. 1991, J. Atmos. Terr. Phys., 53, 1005
Trilling, D. E., Brown, R. H., & Rivkin, A. S., 1999, AAS, DPS Meeting 31, 02.04
Tsuji, T., Ohnaka, K., & Aoki, W. 1999, ApJ, 520, L119
Zirin, H. 1975, ApJ, 199, L63
Zirin, H., & Liggett, M. A. 1982, ApJ, 259, 719

*Note added in proof.*—Mazeh et al. (2000) gives $R_P = 1.4 \pm 0.17 R_J$ and $R_* = 1.2 \pm 0.1\ R_\odot$, corrected from an earlier version quoted in this paper. We have not incorporated these values in this paper, which is meant to be a conceptual description and estimate of CEGP transmission spectra rather than an exact prediction.